

The Specific Case Analysis of Biomineralization Induced by Sulfate Reducing Bacteria

Hongwei Liu¹, Shuang Qin¹, Chaoyang Fu¹, Fei Xiao¹, Deli Wang¹,
Xia Han², Tianli Wang², and Hongfang Liu^{1,†}

¹Hubei Key Laboratory of Materials Chemistry and Service Failure, School of Chemistry and Chemical Engineering, Huazhong University of Science and Technology, Wuhan 430074, China

²Sinopec Oilfield engineering design Corporation, Dongying, 257000, China

(Received November 14, 2017; Revised November 14, 2017; Accepted December 26, 2017)

The effects of sulfate reducing bacteria (SRB) on the corrosion and scaling of the Q235 carbon steel has been investigated in the simulated sewage water and oil field gathering pipelines production water, using scanning electron microscopy (SEM), energy dispersive x-ray spectrometry (EDS), and three-dimensional stereoscopic microscope. Results indicated that the concentration of SRB reached the maximum value on the ninth day in simulated sewage water with a large amount of scaling on the surface of specimen. In oil field gathering pipelines, a large amount of scaling and mineralization of mineral salts and thick deposition of extracellular polymeric substance (EPS) layers were also observed on the surface of specimen. The thickness of biofilm was about 245 μm within 30 days. After adding microbicides, the thickness of corrosion products film was only up to 48 - 106 μm within 30 days, suggesting that SRB could induce biomineralization. Under-deposit corrosion morphology was uniform in the absence of microbicides while local corrosion was observed in the presence of microbicides.

Keywords: SRB, biomineralization, EPS, biofilm, corrosion

1. Introduction

Generally, the term biomineralization refers to biologically controlled mineralization, i.e. mineralization manipulated by the organisms (bacteria, algae *et al.*) and based on genetic [1,2]. Biomineralization is a term used to describe the biologically inspired formation of minerals predetermination. In general, the formation of iron biominerals is not difficult to achieve, bacteria simply provide charged surfaces that bind metals and they excrete metabolic waste products into the surrounding environment that induce mineralization [3].

With the vast majority of bacteria biomineralization is a two-step process: initially metals are electrostatically bound to the anionic surfaces of the cell wall and surrounding organic polymers, where they subsequently serve as nucleation sites for crystal growth [4,5]. The type of biomineral formed is inevitably dependent on the available counter-ions, and hence, the chemical composition of the waters in which the microorganisms are growing [4]. In oxygenated waters, The metabolic activity of Iron Oxidizing

Bacteria (IOB) can induce ferric hydroxide precipitation as a secondary by-product [6]. Ferric hydroxide may then serve as a precursor for more stable iron oxides, such as goethite and hematite via dissolution–reprecipitation or dehydration, respectively, or it may react with dissolved silica, phosphate or sulfate to form other authigenic mineral phases [7]. However, under anoxic conditions, the main products of anaerobic microbial mineralization are calcite and iron sulfide, and lack of siderite. Iron oxide could precipitate and effectively eliminate the negative impact of S^{2-} on the microbial activity. In addition, Ca^{2+} released from the gypsum would react with CO_2 to generate calcite which had a potential application in the area of carbon fixation. Under anoxic conditions, Sulfate Reducing Bacteria (SRB) played a key role in the process of biomineralization [8]. Biomineralization induced by SRB mainly include two aspects: one hand, the sulfide metabolized by SRB can react with dissolved metal cations (e.g. Fe^{2+} , Cu^{2+} , Ni^{2+} et al) to generate precipitate as metal sulfides [8]; on the other hand, the extracellular polymeric substances (EPS) produced by SRB had high complexation with metal ions [9,10]. Calcium binding to EPS has been investigated using various approaches. Using a calcium specific elec-

[†] Corresponding author: liuhf@hust.edu.cn

Table 1 The water quality of Shengli oilfield water pipes

pH	$C_{SRB}/\text{Cells.mL}^{-1}$	Ca ²⁺	Cl ⁻	Fe ²⁺	CO ₂	dissolved oxygen	Total salinity	$V_{\text{corr}}/\text{mm.a}^{-1}$
		mg/L ⁻¹						
7.26	2.5×10^3	295.2	6622.1	1.45	35.2	0.08	11837.7	0.039

trode, calcium binding experiments using EPS from sulfate reducing bacteria isolated from a microbial mat showed that maximum calcium binding capacity could reach 120 - 150 mg Ca per g EPS [9].

In the oil gathering pipelines, some precipitated scales were easily produced, with the parameters change of highly mineralized water, such as pressure and the temperature, especially induced by microorganism (e.g., SRB). Because SRB widely participated in the sulfur cycle in nature [11,12], and beyond the function, SRB also play an important role in global cycling of numerous other elements (e.g., the carbon cycle) [13]. In addition, the EPS produced by SRB also had high complexation for the metal ions. So, SRB not only affected the mineralization, but also influenced the structure of precipitated scale and under-deposit corrosion behavior [14].

In the paper, we made much effort to study the phenomenon of scaling in the oil gathering pipelines. The structure of precipitated scaling and the under-deposit corrosion behavior were investigated in the simulated sewage water and oil field gathering pipelines, which provide technical support for the prevention and control of scaling and corrosion in oil field.

2. Experimental

2.1 Metal samples preparation

The corrosion specimens were cut from Q235 carbon steel sheet, the nominal elemental composition (wt%) of Q235 carbon steel specimens was: C(≤ 0.3), Si(≤ 0.01), Mn(≤ 0.42), S(≤ 0.029), P(≤ 0.01), and Fe balance. In laboratory conditions, the disc shape specimens with a diameter of 15 mm and thickness of 1.5 mm were used for biofilm observation. And, in the Shengli oilfield water pipes, the steel columns with a diameter of 18 mm and height of 30 mm which embedded in the inner wall of oilfield water pipes were also used for biofilm observation. In laboratory conditions, all specimens were abraded through 600, 800 and 1200-grit silicon carbide metal-lurgical paper, degreased in acetone, washed with anhydrous ethanol, then ethanol, dried with nitrogen gas and desiccated until use. All specimens were sterilized by uv lamp for 30 minutes before experiment to ensure there are no other bacteria during experiment.

2.2 Water sample

The water sample was collected from Shengli oilfield water pipes. Samples were taken using a sterile plastic container and then immediately transported to a laboratory for further analysis. The water quality characteristic is described in Table 1.

2.3 Microbiological cultivation and inoculation

Experimental SRB was isolated from soil. In laboratory conditions, the API-RP38 culture medium used in the stagnant batch experiment contained (per liter of distilled water) [15] 4.0 ml sodium lactate, 1.0 g yeast extract, 0.1 g vitamin C, 0.2 g magnesium sulfate ($\text{MgSO}_4 \cdot 7\text{H}_2\text{O}$), 0.01 g potassium diphosphate (K_2HPO_4) and 10.0 g sodium chloride. The pH was adjusted to 7.0-7.2 by the addition of 1 mol·l⁻¹ NaOH solution. The culture medium was purged with pure nitrogen gas for thirty minutes to assure anaerobic environments for SRB. And the culture medium, test cells and associated tubes were then sterilized in an autoclave at 121 °C for 20 min and then cooled to room temperature. After cooling, 0.2g $\text{Fe}(\text{NH}_4)_2\text{SO}_4 \cdot 6\text{H}_2\text{O}$, which had been sterilized by ultraviolet light for 20 min, was added to the medium. Test cells were inoculated with 10% (v/v), and SRB cultures were incubated at 37 °C. The number of active SRB (NSRB) value in the system was calculated in most probable number (MPN) method [16] according to the American Society of Testing Materials (ASTM) Standard D4412-84.

2.4 Surface analysis

The test coupons were examined for surface biofilm and corrosion features using Scanning electron microscopy (SEM) and Energy dispersive X-ray spectrometry (EDS). The surface behavior and element distribution of mild steel coupons with biofilm immersed in different corrosion conditions with time were observed using JEOL JSM 35 °C SEM at an accelerating voltage of 20.0 kV. The morphology of coupons was observed and analyzed by three-dimensional stereoscopic microscope. The three-dimensional stereogram was carried to analyze the thickness of biofilm.

Prior to observation of the morphology of coupons, the coupons removed from medium, rinsed in pickling solution containing corrosion inhibitor to remove corrosion

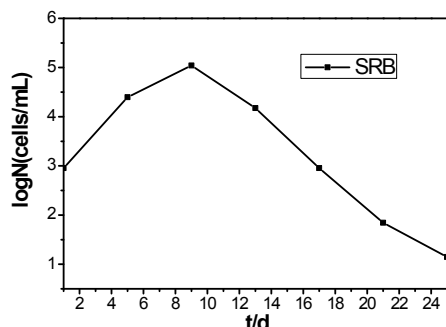


Fig. 1 The free floating SRB growing process in sewage of oil-field.

products, followed by rinsing with acetone and sterile de-ionized water, then dried in nitrogen flow. Before SEM observation of biofilm, the steel was pretreated by soaking the steel overnight on 2.5% glutaraldehyde in phosphate buffer solution for 8 hours [17]. The steels were then dehydrated using serial dilution of ethanol (10%, 30%, 50%, 70%, 90%, 95% and 100%), each for 10 minutes, the final step for 30 minutes. Afterwards all the cylinder steels were dried using nitrogen and placed in desiccators.

3. Results

3.1 Laboratory studies on biofilm

3.1.1 The growth curves of srb

The concentration of SRB in the sewage of oil-fields was 2.5×10^3 cells. ml^{-1} (Table 1) which indicated that SRB can survive in the sewage. After inoculated with 1% (v/v) SRB in the sewage, the growing process of free floating SRB was as shown in Fig. 1. During inoculation 10 days, the number of active SRB increases quickly and

the number of SRB achieves the maximum value at the 10th day. In the stage, the activity of SRB was relatively high, and accelerating the growing of biofilm. At the 10th day, the biofilm tend to mature. After 10th day, the concentration of SRB gradually tend to dead due to the consumption of nutrients. Meanwhile, the surface of carbon steel could produce local corrosion with the rupture of biofilm.

3.1.2 The analysis of morphology of carbon steels surface

Fig. 2 shows the results of SEM and EDS analysis of the SRB biofilms that developed on Q235 steels that was immersed in sewage with different time. The different surface morphology of biofilms of carbon steels appeared with time, and the growing of biofilm had special features as dynamic and harmonious (Fig. 2a and b). After 8 days, a layer of dense biofilm with a large amount of viscous flakes was observed on the surface of the steel (Fig. 2a) which can due to SRB in the internal biofilm entered into vigorous growth and metabolism period, then produced a large amount of viscous EPS (Fig. 2 a) that insured the stability of biofilm that in accordance with the free floating SRB growing process (Fig. 1). After 20 days, the morphology of biofilm was complex that partly was covered by sheets which could protect substrate, and partly was covered by a small amount of scale which could induce biomineralization by SRB.

Table 2 shows the analysis results of EDS of biofilm after exposed to sewage 8 days and 20 days. After 8 days, a large amount of elements C and O were observed on the surface of biofilm, which indicated that the biofilm was composed of a large amount of EPS, and may account for the incorporation of metals (e.g. Fe, Ca, Mg) [18]. Furthermore, the EPS can effect on the mineralization and

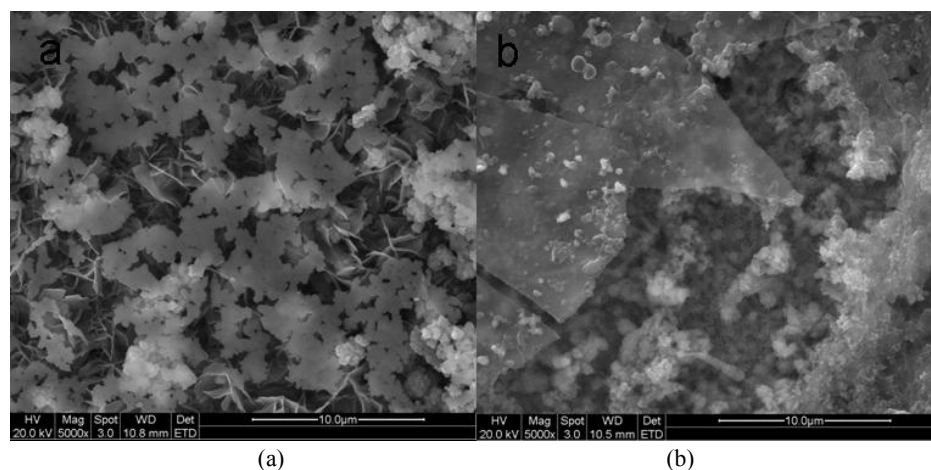


Fig. 2 SEM analysis of biofilm on Q235 steel coupons after exposed to sewage with different time (a, 8d; b, 20d).

Table 2 The analysis results of EDS of biofilm after exposed to sewage for 8 days and 20 days

Element	C	O	Si	P	S	Fe
8d (at%)	90.57	6.18	1.32	-	0.83	1.10
20d (at%)	60.65	8.65	1.34	0.33	0.48	28.55

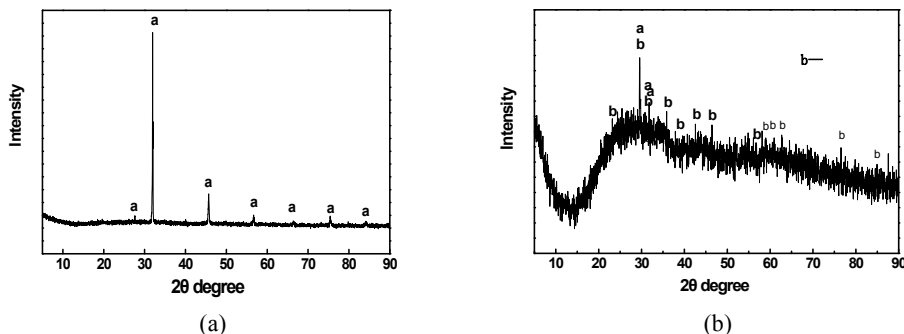


Fig. 3 XRD for the surface of Q235 carbon steels immersed in sewage containing SRB (a) and sterile sewage (b) after 11 days [19].

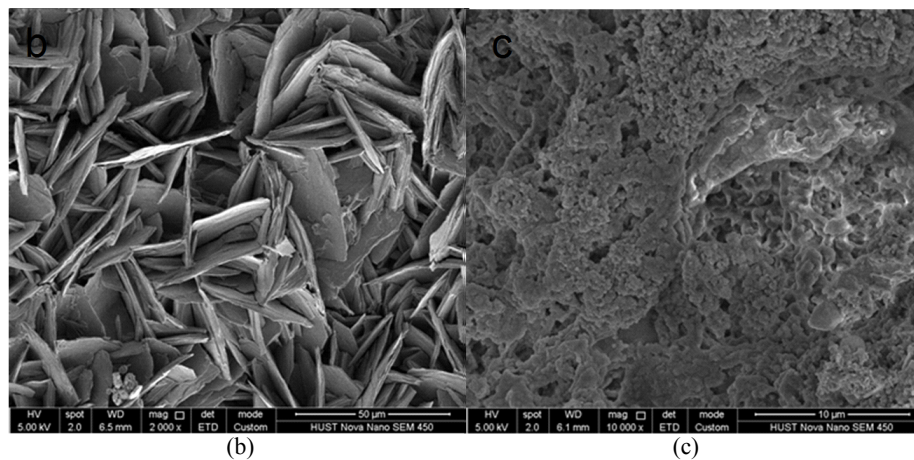
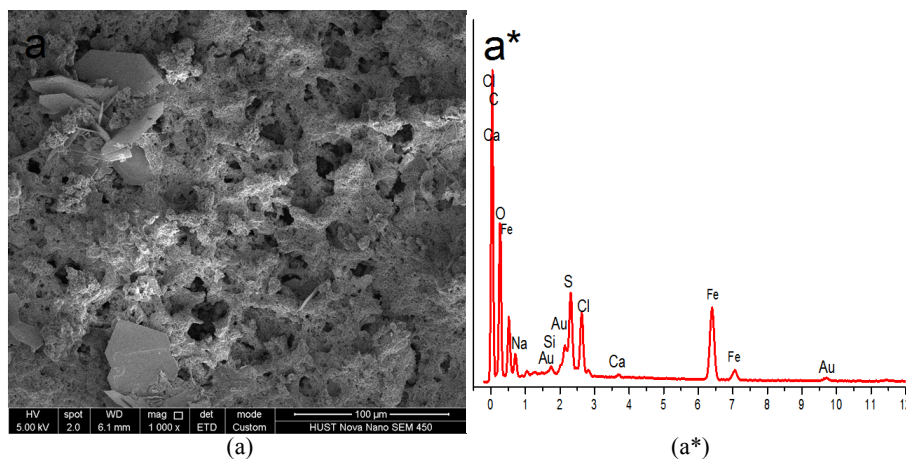


Fig. 4 SEM and EDS analysis of biofilm on the surface of shell of pipe specimen for 30 days (a, the region of total morphology of biofilm; a*, the EDS analysis of biofilm; b, the region of scaling and mineralization of mineral salts; c, the main region of EPS cover) [20].

Table 3 The analysis results of EDS of biofilm on the surface of shell of pipe specimen after 30 days

Element	CK	OK	SK	NaK	SiK	CaK	ClK	FeK
at%	69.94	16.91	2.86	0.42	0.26	0.84	2.59	5.79

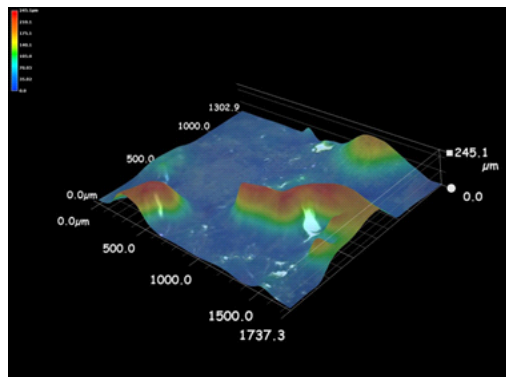


Fig. 5 The three-dimensional stereogram of biofilm after 30 days.

scale precipitation. After 20 days, the main elements on the biofilm include C, O, Si, P, S, and Fe, which may suggest the formation of inorganic mineral compounds. However due to the existence of SRB, a large amount of organics covered the biofilm surface.

3.1.3 The analysis of crystal phase of carbon steels surface

In the presence of SRB, the surface of carbon steel gradually formed a compact biofilm layer which contained plenty of ferrous sulfide crystals that possessed complete crystal shape (Fig. 3a). However in the sterile sewage, very weak diffraction peaks was found and only a small amount of CaCO_3 and $\text{Ca}_2\text{P}_2\text{O}_7$ with low degree of crystal-

linity (Fig. 3b) that produced by the mineralization of high total salinity water was formed on the carbon steel surface. In addition, a large amount of amorphous substances that could be seen by naked eyes covered completely on the carbon surface.

3.2 Oil field studies on biofilm

3.2.1 The analysis of morphology of carbon steels surface

Fig. 4 shows the main SEM micrographs of the surface of shell of pipe specimen for 30 days. After a period of 30 days, a thick biofilm layer with pores all over the surface of specimen was noticed (Fig. 4a). And mineral scale inhibition which might be caused by synergistic effect of SRB and mineralization induced by inorganic salts were covered the completely surface of specimen. In other region, a large amount of scaling and mineralization of mineral salts which present block crystal can be seen clearly (Fig. 4b), that indicate the true mineralization in the shell of pipe in oil field. However, in another region, thick deposition of EPS layers was noticed that showed a large amount of high metabolism active SRB existed inside of biofilm (Fig 5c). Further, the complexation between EPS and metal ions promoted the biomineralization.

The results of EDS of biofilm also agree with the SEM analysis (Table 3). The main elements on the biofilm include C, O, S, Si, Ca, Fe, et al (Table 3), which may

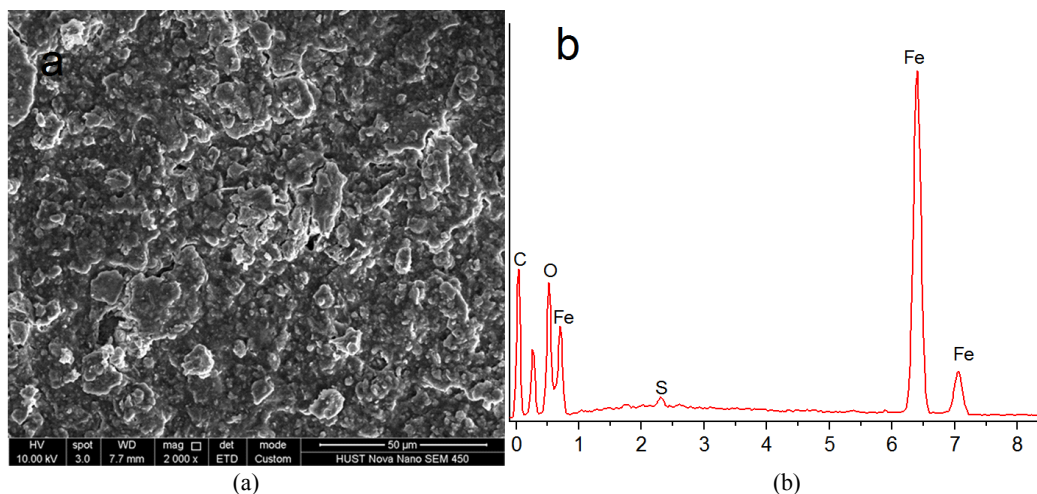


Fig. 6 SEM and EDS analysis of biofilm on the surface of shell of pipe specimen for 8 days (a, the region of total morphology of biofilm; b, the EDS analysis of biofilm).

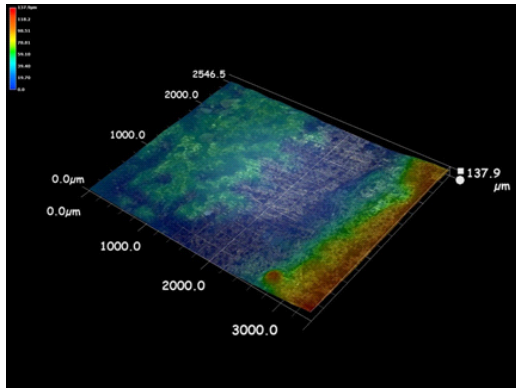


Fig. 7 The three-dimensional stereogram of biofilm after 8 days.

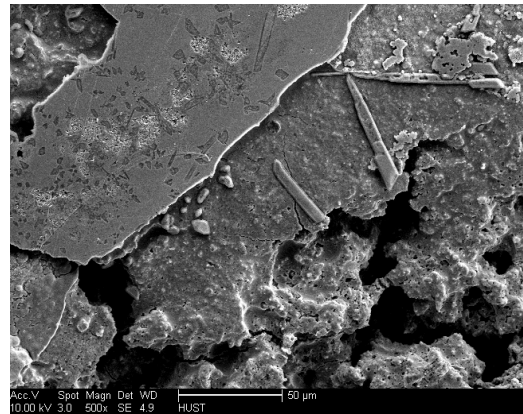


Fig. 8 SEM analysis of biofilm on the surface of shell of pipe specimen with adding microbicide for 30 days.

Table 4 The analysis results of EDS of biofilm on the surface of shell of pipe specimen after 8 days

Element	C	O	S	Fe
at%	39.92	23.09	0.56	36.43

Table 5 The analysis results of EDS of biofilm on the surface of shell of pipe specimen with adding microbicide after 30days

Elements	C	O	S	Fe
at%	15.81	49.73	1.41	33.05

suggest the formation of a large amount of EPS and inorganic mineral compounds.

These results acquired by oil field experiment also consistent with the results come from laboratory studies

As shown in Fig. 5, the thickness of biofilm was about 245 μm. The inhomogeneity in thickness of biofilm may mainly was induced by ability of SRB adhere to different regions of specimen and the difference of metabolism activity of SRB existed in biofilm internal.

Fig. 6 showed SEM and EDS analysis of biofilm on the surface of shell of pipe specimen for 8 days. Since the specimen was taken after 8 day exposure and kept in the air, it directly induced the rupture of biofilm and corrosion products by oxidation (Fig. 6a). The results of EDS of biofilm suggest the existence of SRB and EPS (Fig. 6b and Table 4). The thickness of biofilm was about up to 138 μm (Fig. 7) in only 8 days.

These analysis results also suggested that SRB may induce the biomineralization.

3.2.2 Studies on biofilm with adding microbicides

As shown in the Fig. 8, after adding microbicide, the specimen surface was covered with heavily mineralized multilayered lump (Fig. 8) that may attributed to the mineralization of inorganic salts because of the dead of lots of SRB. However, in the local region, we still observed the existence trace of EPS (Fig. 8). And the results of EDS indicated that the main elements include C, O, S and Fe (Table 5), which also proved the existence of SRB

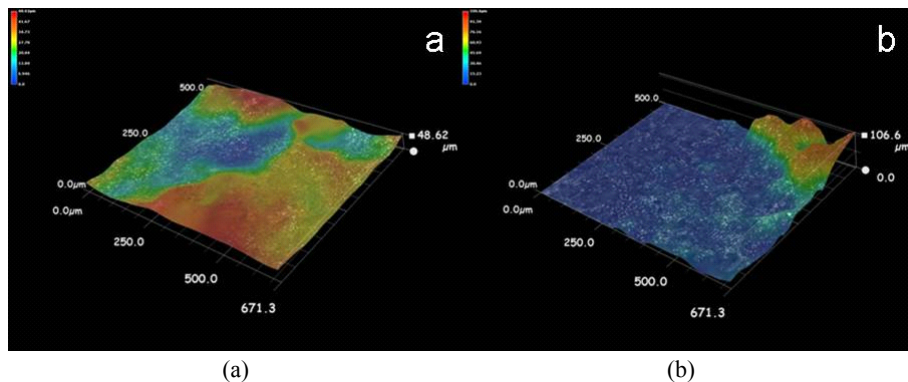


Fig. 9 The three-dimensional stereogram of biofilm (a and b were the different typical regions of specimen) Analysis of corrosion morphology.

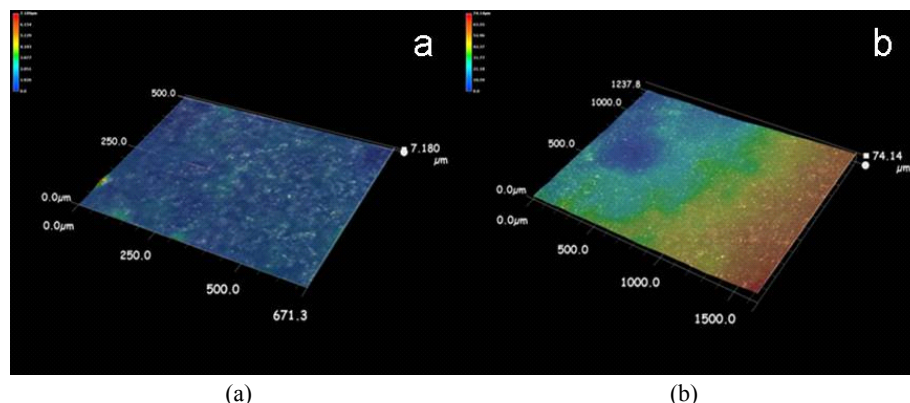


Fig. 10 The three-dimensional stereogram of corroded surface after the removal of corrosion - products (a, without microbicide; b, with microbicide).

in the region. But, the less content of carbon in the region (Table 5) suggest that only a small amount of survival SRB, and the main corrosion products was iron oxide (Table 5).

As shown in the Fig. 9, the surface of specimen was not relative uniform, and the thickness of corrosion products film was only up to 48-106 μm (Fig. 9) in 30 days, which only almost half of the thickness of biofilm that induced by SRB.

Synthesize the above results; we can conclude that SRB played a key role in the mineralization of gathering pipeline in oilfield.

As shown in the Fig. 10, after the corrosion products were removed, the surface of specimen was relative uniform and the corrosion of specimen was mainly uniform corrosion in the absence of microbicide. However, in the absence of microbicide, with lighter local corrosion was observed on the surface of specimen, and the maximum corrosive pit depth was 20 μm (Fig. 10).

4. Discussion

4.1 Analysis of biofilm components

In the laboratory studies, at shorter incubation times (8 days), a large amount of organics covered the surface of carbon steel (Fig. 2a) which attributed to faster growth rates of SRB, meanwhile, a large amount of EPS were produced by SRB [21]. And at longer incubation times (20 days) (Fig. 2b), the component of biofilm differed from the 8 days that the inorganics content of biofilm increased (Table 2). In addition, different from the 8 days, sheets and scale covered the carbon steel surface (20 days) (Fig. 2b). Meanwhile, a large amount of iron sulfide formed by the reaction of iron oxide in the rust and hydrogen sulfide produced by SRB [22], and accompanied with

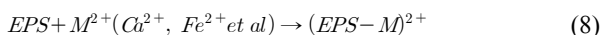
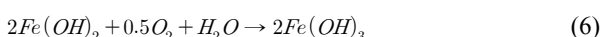
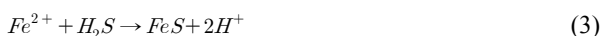
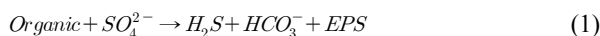
the complexation between EPS and metal cations [21]. However, in the oil field studies, at longer incubation times (30 days), a large amount of organic and inorganic mineral compounds were found on the surface of specimen (Fig. 5) different from the laboratory studies which may due to low concentration of SRB and the fluid flow condition influence in the pipeline, resulting in the low yield and EPS and partly inorganic mineralization [23]. But, in all process, SRB played a key role [24,25]. After adding microbicide, some SRB interior biofilm survived, resulting the increase of sulfur content in the local regions (Fig. 8 and Table 5). In the most regions of specimen, the specimen surface was covered with heavily mineralized multilayered lump (Fig. 8), indicating that almost no SRB existed in the oilfield water pipes.

4.2 Analysis of biomineralization process

As we know, one hand, SRB induced mineralization is a direct result of microbial activities, which generate the biochemical conditions necessary to facilitate sulfide precipitation; on the other hand, SRB induced mineralization is a passive process that a result of interactions between EPS and metal cations (e.g., Fe^{2+} , Ca^{2+} , Mg^{2+}) [23,26]. In the oil field studies, at longer incubation times (30 days), the thickness of biofilm induced by SRB was over twice as much as the thickness of biofilm induced by little SRB that were not killed by microbicide (Fig. 5 and Fig. 9), indicating SRB played an important role in the process of mineralization of oilfield water. The results also coincide with above the process of SRB induced mineralization.

On the basis of all the above analysis, we can concluded the whole process of biomineralization induced by SRB as follows [1,10,26]: (1) Preparation of biomineralization: SRB grew and metabolized fast, produced, Fig. 5 and

Table 4). SRB could promote or inhibit crystal nucleation by changing the saturation index for carbonate silicates, phosphates and so on, i.e. SRB could affect the amount of EPS, carbonate, silicates, phosphate et al available for complexation with metal cations (e.g., Fe^{2+} , Ca^{2+} , Mg^{2+}) [9,27,28]. Chemical and biological equations were listed as follows:



4.3 Analysis of under-deposit corrosion behavior

After the corrosion products were removed, the surface of specimen was relative uniform and the corrosion of specimen was mainly uniform corrosion (Fig. 10a) which may due to the mounts of SRB covered the almost all surface of specimen and the activity of SRB was high in the absence of microbicides. However, in the presence of microbicides, the corrosion of specimen was light and local corrosion was observed. The reasons were mainly include two aspects: one hand, the thicker biofilm hindered the corrosive ions which had the protective effect for specimen; on the other hand, the scale deposit in pipelines provided protective effect for SRB under the biofilm, and thus enhanced the local corrosion.

5. Conclusions

Under the condition of laboratory experiments on biofilm, in the presence of SRB, the surface of specimen covered a large amount of FeS and EPS, and in the sterile sewage, only a small amount of $CaCO_3$ and $Ca_2P_2O_7$ with low degree of crystallinity was formed on the specimen surface and a large amount of amorphous substances were observed.

Under the condition of oil field experiments on biofilm, a large amount of scaling and mineralization of mineral salts and thick deposition of EPS layers with SRB were observed on the surface of specimen, And the analysis results of EDS indicated that the main elements on the

biofilm include C, O, S, Si, Ca, Fe. However, after adding microbicides in the pipeline, the specimen surface was covered with heavily mineralized multilayered lumps. And the results of EDS indicated that the main elements include C, O, Fe and with little S. The thickness of biofilm was about 245 μm and 48 - 106 μm in the absence of microbicides and presence of microbicides, respectively, which suggested that SRB enhanced the biomineralization. After the corrosion products were removed, uniform corrosion and local corrosion were observed in the absence of microbicides and presence of microbicides, respectively.

Acknowledgements

This research was supported by the National Natural Science Foundation of China (51171067), the Natural Science Foundation of Shenzhen City (JC201005310696A). We acknowledge the support of the Analytical and Testing Center of the Huazhong University of Science and Technology.

References

1. H. A. Lowenstam and S. Weiner, *On biomineralization*, pp. 1 - 336, Oxford University Press, UK (1989).
2. L. Addadi, S. Raz, and S. Weiner, *Adv. Mater.*, **15**, 959 (2003).
3. S. Weiner and P. M. Dove, *Rev. Mineral. Geochem.*, **54**, 1 (2003).
4. K. O. Konhauser, *Earth Sci. Rev.*, **43**, 91 (1998).
5. K. L. Gallagher, C. Dupraz, O. Braissant, R. S. Norman, A. W. Decho, and P. T. Visscher, *Mineralization of sedimentary biofilms: modern mechanistic insights in Biofilm: Formation, Development and Properties*, Chapter 6, pp. 1 - 33, Nova Science, New York (2010).
6. D. Emerson, E. J. Fleming, and J. M. McBeth, *Annu. Rev. Microbiol.*, **64**, 561 (2010).
7. J. Miot, K. Benzerara, G. Morin, A. Kappler, S. Bernard, M. Obst, C. Féraud, F. Skouri-Panet, J.-M. Guigner, N. Posth, M. Galvez, G. E. Brown Jr., and F. Guyot, *Geochim. Cosmochim. Ac.*, **73**, 696 (2009).
8. J. F. Heidelberg, R. Seshadri, S. A. Haveman, C. L. Hemme, I. T. Paulsen, J. F. Kolonay, J. A. Eisen, N. Ward, B. Methe, L. M. Brinkac, S. C. Daugherty, R. T. Deboy, R. J. Dodson, A. S. Durkin, R. Madupu, W. C. Nelson, S. A. Sullivan, D. Fouts, D. H. Haft, J. Selengut, J. D. Peterson, T. M. Davidsen, N. Zafar, L. Zhou, D. Radune, G. Dimitrov, M. Hance, K. Tran, H. Khouri, J. Gill, T. R. Utterback, T. V. Feldblyum, J. D. Wall, G. Voordouw and C. M. Fraser, *Nat. Biotechnol.*, **22**, 554 (2004).
9. O. Braissant, A. W. Decho, C. Dupraz, C. Glunk, K. M. Przekop, and P. T. Visscher, *Geobiology*, **5**, 401 (2007).
10. A. Spadafora, E. Perri, J. A. McKenzie, and C. Vasconcelos, *Sedimentology*, **57**, 27 (2010).
11. M. Labrenz, G. K. Druschel, and T. Thomsen-Ebert,

- Science*, **290**, 1744 (2000).
12. Y. Shen, R. Buick, and D. E. Canfield, *Nature*, **410**, 77 (2001).
 13. A. Müller and B. Krebs, *Sulfur: Its Significance for Chemistry, for the Geo-, Bio-, and Cosmosphere and Technology; Studies in Inorganic Chemistry*, Book 5, pp. 1 - 526, Elsevier Science Ltd., Amsterdam (1984).
 14. B. Little, P. Wagner, K. Hart, R. Ray, D. Lavoie, K. Nealson, and C. Aguilar, *Biodegradation*, **9**, 1 (1998).
 15. E. I. Sungur and A. Cotuk, *Environ. Monit. Assess.*, **104**, 211 (2005).
 16. H. A. Videla, *Manual de Biocorrosion*, pp. 1 - 304, CRC Press, Florida (1996).
 17. M. J. Hernández Gayosso, G. Zavala Olivares, N. Ruiz Ordaz, C. Juárez Ramirez, R. García Esquivel, and A. Padilla Viveros, *Electrochim. Acta*, **49**, 4295 (2004).
 18. A. Spadafora, E. Perri, C. Vasconcelos, and J. A. Mckenzie, *Proc. European Geosciences Union Conf.*, Vienna, Austria (2008).
 19. Q. Ye, K. J. Li, P. P. Guo, and H. F. Liu, *Corros. Sci. Protect. Technol.*, **25**, 195 (2013).
 20. H. W. Liu, H. F. Liu, S. Qin, X. Han, and T. Wang, *Corros. Sci. Protect. Technol.*, **1**, 7 (2015).
 21. Z. H. Dong, T. Liu, and H. F. Liu, *Biofouling*, **27**, 487 (2011).
 22. J. Duan, S. Wu, X. Zhang, G. Huang, M. Du, and B. Hou, *Electrochim. Acta*, **54**, 22 (2008).
 23. A. W. Decho, *Ecol. Eng.*, **36**, 137 (2010).
 24. B. J. Little, F. B. Mansfeld, P. J. Arps, and J. C. Earthman, *Microbiologically Influenced Corrosion*, Wiley Online Library, Wiley, New York (2007).
 25. G. M. Gadd, *Curr. Opin. Biotechnol.*, **11**, 271 (2000).
 26. S. Mann, *Biomaterialization: Principles and Concepts in Bioinorganic Materials Chemistry*, vol. 5, pp. 1 - 210, Oxford University Press, New York (2001).
 27. A. Soetaert, T. Vandenbrouck, K. van der Ven, P. Van Remortel, R. Blust, and W. M. de Coen, *Aquat. Toxicol.*, **83**, 212 (2007).
 28. C. Dupraz, R. P. Reid, O. Braissant, A. W. Decho, R. S. Norman, and P. T. Visscher, *Earth Sci. Rev.*, **96**, 141 (2009).